International Journal of Heat and Mass Transfer 170 (2021) 120993

Contents lists available at ScienceDirect

International Journal of Heat and Mass Transfer

journal homepage: www.elsevier.com/locate/hmt

Imaginary Eigenvalues in Multilayer One-Dimensional Thermal Conduction Problem with Linear Temperature-Dependent Heat Generation

Ankur Jain[a,*], Mohammad Parhizi[a], Long Zhou[b], Girish Krishnan[a]

[a] Mechanical and Aerospace Engineering Department University of Texas at Arlington, Arlington, TX, USA
[b] School of Mechanical and Power Engineering, Henan Polytechnic University, Jiaozuo, Henan, China.

ARTICLE INFO

Article history:
Received 7 December 2020
Revised 2 January 2021
Accepted 13 January 2021

Keywords:
Diffusion
Multilayer Body
Eigenvalues
Imaginary Numbers
Li-ion Cells

ABSTRACT

Diffusion in a multi-layer body is a common problem in heat and mass transfer, with applications in multiple engineering systems, such as Li-ion battery packs and first-order chemical reactions occurring in a multilayer body. Development of analytical models to describe diffusion in such systems is helpful for both heat and mass transfer. This paper addresses a multi-layer one-dimensional diffusion problem, in which, generation/consumption in each layer is proportional to the local temperature/concentration. This could occur, for example, due to temperature-dependent heat generation or species generation/consumption associated with a first-order chemical reaction. It is shown that eigenvalues of this problem may become imaginary under two distinct conditions. A physical interpretation of these conditions is discussed, and a mathematical requirement for existence of imaginary eigenvalues is derived. The relationships between imaginary eigenvalues and various non-dimensional problem parameters are discussed. It is also shown that the computed temperature in the multilayer body remains real even if some eigenvalues may become imaginary. Therefore, all eigenvalues, whether real or imaginary must be accounted for in temperature computation. While presented in the context of heat transfer, these results are also valid for multi-layer mass transfer problems involving species generation/consumption due to chemical reaction. This work improves the theoretical understanding of diffusion in a multilayer body under conditions relevant for several engineering processes and systems.

1. Introduction

Thermal conduction in multilayer bodies is of significant theoretical and practical importance [1–3]. Several multilayer engineering systems comprise multiple heterogeneous layers, and the nature of thermal conduction through the layers directly impacts performance and safety. A few examples of such multilayer systems include Li-ion cells [4], microelectronics [5], nuclear engineering components [6] and civil engineering structures [7].

While several methods exist for the theoretical analysis of thermal conduction in a multilayer body, including complex variables [8] and adjoint method [9], the separation of variables method using quasi-orthogonal eigenfunctions [10,11] has been used most commonly. In this technique applied to a problem with homogeneous boundary conditions and no heat generation, temperature distribution in each layer is expressed as an infinite series, usually with the same time term. This makes it possible to satisfy the interface conditions by appropriately choosing the coefficients appearing in the spatial terms. Specifically, the eigenvalues of the problem are derived by requiring the system of homogeneous equations comprising the boundary and interface conditions to admit a non-trivial solution, which, mathematically, requires the determinant of the system of equations to be zero. The remaining coefficient in the solution is determined by using the initial condition and quasi-orthogonality applied over the entire geometry, using weighing parameters unique for each layer. Non-homogeneities in the boundary conditions or in the governing equation itself are handled by splitting the solution into multiple parts. Advanced problems such as those involving thermal contact resistance between layers [12], spatially-dependent convective boundary conditions [13], time-dependent convective boundary conditions [14], two-dimensional multilayer bodies [15], etc. have also been presented.

* Corresponding Author.
E-mail address: jaina@uta.edu (A. Jain).

https://doi.org/10.1016/j.ijheatmasstransfer.2021.120993
0017-9310/

Nomenclature

Bi	Biot number
h	convective heat transfer coefficient ($Wm^{-2}K^{-1}$)
i	unit imaginary number, $i = \sqrt{-1}$
k	thermal conductivity ($Wm^{-1}K^{-1}$)
$\bar{k}$	non-dimensional thermal conductivity
M	number of layers
N	eigenvalue norm
T	temperature (K)
x	spatial coordinate (m)
t	time (s)
α	diffusivity (m^2s^{-1})
$\bar{\alpha}$	non-dimensional diffusivity
β	source coefficient (s^{-1})
$\bar{\beta}$	non-dimensional source coefficient
γ	non-dimensional interface location
τ	non-dimensional time
θ	non-dimensional temperature
ω	non-dimensional eigenvalue
ξ	non-dimensional spatial coordinate
λ	non-dimensional eigenvalue
Subscripts	
m	layer number
0	initial value

Literature suggests that thermal conduction in a multi-dimensional, multi-layer body may lead to imaginary eigenvalues [16–18]. Imaginary eigenvalues have been reported in the past for 2D [16,17] and 3D multilayer problems [18]. A limited amount of work on 1D multilayer bodies [19] also suggests the existence of imaginary eigenvalues, although a detailed interpretation and analysis is missing. Past work on 2D and 3D bodies offers useful guidelines for the regimes of property values in which eigenvalues may become imaginary [15,16] and physical interpretation of this effect [17]. While it has generally been recognized that imaginary eigenvalues must be included in temperature computation, a formal proof that the computed temperature distribution remains real despite imaginary eigenvalues is missing.

The present work considers a diffusion problem in a one-dimensional multilayer body, in which, volumetric generation/consumption in each layer is linearly proportional to the local temperature/concentration. The problem is discussed in the context of thermal conduction, but is equally valid for mass transfer involving species generation/consumption due to chemical reaction. Such scenarios may be relevant for several engineering applications. For example, in a multilayer body where some or all layers undergo a chemical reaction with first-order kinetics, the rate of generation/consumption of a species is proportional to the local concentration [20]. As another example, heat generation in a Li-ion cell is a function of the local temperature [21]. While the general relationship between heat generation rate and local temperature is exponential in nature according to Arrhenius reaction kinetics [21], a linearization is often carried out as a first-order approximation [22]. In such a case, the energy conservation equation contains a heat generation term that is proportional to the local temperature. In these and other related scenarios, it is critical to solve the multilayer problem with temperature/concentration-dependent source term.

This paper shows that for a one-dimensional multilayer body with linear, temperature-dependent heat generation/consumption in various layers, the eigenvalues of the problem may become imaginary under two specific conditions, one of which results in exponential temperature rise over time. The impact of various problem parameters on the appearance of imaginary eigenvalues is analyzed. It is also proved that even when some eigenvalues may become imaginary, the predicted temperature distribution remains real. As a result, it is critical to consider all eigenvalues, whether real or imaginary. The next section defines the problem, including non-dimensionalization and presents an analytical solution. The conditions under which imaginary eigenvalues may occur and the impact on the temperature distribution is discussed in subsequent sections.

2. Problem Definition and Derivation of Solution

Consider diffusion-based, continuum thermal conduction in a general, one-dimensional, M-layer body, as shown in Figure 1. General, convective boundary conditions are considered at the two ends of the body. Volumetric heat generation proportional to the local temperature occurs in each layer. A non-zero initial temperature distribution is assumed. Other non-homogeneities, such as heat flux boundary condition or constant heat generation within any layer are assumed to already have been accounted for by appropriately splitting up the problem into multiple sub-problems, as discussed in standard textbooks [1,2]. Mathematically, the problem can be defined as

$$\frac{\partial T_m}{\partial t} = \alpha_m \frac{\partial^2 T_m}{\partial x^2} + \beta_m T_m (m = 1, 2, 3 \ldots M) \tag{1}$$

where $\beta_m T_m$ represents a source term that is proportional to the local temperature. β_m is referred to as the source coefficient and has units of s^{-1}. Positive or negatives values of β_m correspond to heat generation or consumption, respectively. The case of positive β_m is of particular interest because it represents positive feedback between temperature and heat generation – as temperature goes up, so does heat generation, which further increases temperature, potentially leading to thermal runaway.

The associated boundary conditions are

$$-k_1 \frac{\partial T_1}{\partial x} + h_A T_1 = 0 \ at \ x = 0 \tag{2}$$

$$k_M \frac{\partial T_M}{\partial x} + h_B T_M = 0 \ at \ x = x_M \tag{3}$$

It is assumed that at least one of the convective heat transfer coefficients h_A and h_B is non-zero. In addition, based on perfect thermal contact and heat flux conservation between layers, the following interface conditions are assumed to exist between layers:

$$T_m = T_{m+1} \quad at \ x = x_m \tag{4}$$

$$k_m \frac{\partial T_m}{\partial x} = k_{m+1} \frac{\partial T_{m+1}}{\partial x} \quad at \ x = x_m \tag{5}$$

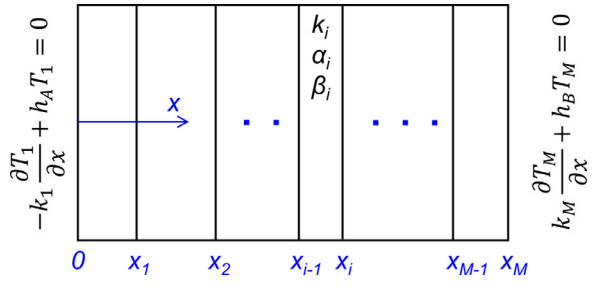

Fig. 1. Schematic of the one-dimensional multilayer body with linear, temperature-dependent heat generation in each layer and convective boundary conditions at the two ends.

Eqs. (4) and (5) apply for m=1,2,3..M-1. The initial condition is given by $T_m = T_{m,0}(x)$ at t=0.

The governing equations are scaled prior to seeking a solution. The following variables are introduced: $\theta_m = \frac{T_m}{T_{ref}}, \cdot\xi = \frac{x}{x_M}, \cdot\tau = \frac{\alpha_M t}{x_M^2}, \cdot\gamma_m = \frac{x_m}{x_M}, \cdot\bar{k}_m = \frac{k_m}{k_M}, \cdot\bar{\alpha}_m = \frac{\alpha_m}{\alpha_M}, \cdot\bar{\beta}_m = \frac{\beta_m x_M^2}{\alpha_M}, \cdot\theta_{m,0} = \frac{T_{m,0}}{T_{ref}}, \cdot Bi_A = \frac{h_A x_M}{k_M}, \cdot Bi_B = \frac{h_B x_M}{k_M}$

The non-dimensional set of governing equations obtained by introducing these scaling parameters is

$$\frac{\partial\theta_m}{\partial\tau} = \bar{\alpha}_m \frac{\partial^2\theta_m}{\partial\xi^2} + \bar{\beta}_m\theta_m (m = 1, 2, 3 \ldots M) \tag{6}$$

Subject to

$$-\bar{k}_1 \frac{\partial\theta_1}{\partial\xi} + Bi_A\theta_1 = 0 \ at \ \xi = 0 \tag{7}$$

$$\frac{\partial\theta_M}{\partial\xi} + Bi_B\theta_M = 0 \qquad at \ \xi = 1 \tag{8}$$

$$\theta_m = \theta_{m+1} \quad at \ \xi = \gamma_m \tag{9}$$

$$\bar{k}_m \frac{\partial\theta_m}{\partial\xi} = \bar{k}_{m+1} \frac{\partial\theta_{m+1}}{\partial\xi} \quad at \ \xi = \gamma_m \tag{10}$$

The initial condition is given by

$$\theta_m = \theta_{m,0}(\xi) at \tau = 0 \cdot (m = 1, 2, \cdots M) \tag{11}$$

Note that $\bar{\beta}_m = 0$ reduces this to a standard multilayer thermal conduction problem, with a solution based on quasi-orthogonal eigenfunctions available in textbooks [1,2].

A solution for Eqs. (6)-(11) may be obtained by assuming the following series form:

$$\theta_m(\xi, \tau) = \sum_{n=1}^{\infty} c_n [A_{m,n} \cos(\omega_{m,n}\xi) + B_{m,n} \sin(\omega_{m,n}\xi)] \exp\left(-\lambda_n^2\tau\right) (m = 1, 2..M) \tag{12}$$

where the same exponential term is chosen in each layer in order to help satisfy the interface conditions. Substituting Eq. (12) in the governing equation given by Eq. (6), the eigenvalues $\omega_{m,n}$ and λ_n are shown to be related to each other as follows:

$$\omega_{m,n} = \sqrt{\frac{\lambda_n^2 + \bar{\beta}_m}{\bar{\alpha}_m}} (m = 1, 2 \ldots M) \tag{13}$$

In general, $\bar{\beta}_m$ can be either negative or positive, representing consumption or generation, respectively. Therefore, when λ_n is real, Eq. (13) indicates that the eigenvalues $\omega_{m,n}$ may become imaginary if $\bar{\beta}_m$ is negative and large in magnitude, specifically if $\lambda_n^2 < -\bar{\beta}_m$. Further, as shown in Section 3, λ_1 itself may become imaginary under certain conditions, which may also result in imaginary $\omega_{m,n}$ if $\bar{\beta}_m$ is positive and small in magnitude, such that $\bar{\beta}_m < -\lambda_1^2$.

It is particularly important to understand the implications of imaginary eigenvalues in the present problem. An imaginary value of λ_1 will result in exponentially increasing temperature at large times due to divergence of the exponential term in Eq. (12). Therefore, it is important to predict the conditions in which λ_1 may become imaginary for better understanding thermal runaway in systems such as Li-ion cells. In order to understand when imaginary eigenvalues may occur in the present problem and how the solution may be affected, the eigenequation and subsequent solution for $\theta_m(\xi, \tau)$ is derived next. A special case of the resulting equations for a two-layer body is discussed in the next section.

Eq. (12) is inserted in the boundary and interface conditions given by Eqs. (7)-(10) to obtain

$$-\bar{k}_1\omega_{1,n}B_{1,n} + Bi_A A_{1,n} = 0 \tag{14}$$

$$\bar{k}_M\omega_{M,n}[-A_{M,n}\sin\omega_{M,n} + B_{M,n}\cos\omega_{M,n}] + Bi_B[A_{M,n}\cos\omega_{M,n} + B_{M,n}\sin\omega_{M,n}] = 0 \tag{15}$$

$$A_{m,n}\cos(\omega_{m,n}\gamma_m) + B_{m,n}\sin(\omega_{m,n}\gamma_m) = A_{m+1,n}\cos(\omega_{m+1,n}\gamma_m) + B_{m+1,n}\sin(\omega_{m+1,n}\gamma_m) \tag{16}$$

$$\bar{k}_m\omega_{m,n}[-A_{m,n}\sin(\omega_{m,n}\gamma_m) + B_{m,n}\cos(\omega_{m,n}\gamma_m)] = \bar{k}_{m+1}\omega_{m+1,n}[-A_{m+1,n}\sin(\omega_{m+1,n}\gamma_m) + B_{m+1,n}\cos(\omega_{m+1,n}\gamma_m)] \tag{17}$$

where the relationship between $\omega_{m,n}$ and λ_n is given by Eq. (13).

In general, Eqs. (14)-(17) represents a set of 2M homogeneous equations in 2M variables. In order to ensure a non-trivial solution, the determinant of this set of equations must be zero, which provides the eigenequation to determine the eigenvalues λ_n. Due to the subsequent redundancy in the set of equations, one of the coefficients, usually $A_{1,n}$ is chosen to be 1 [1,2], while the other coefficients are determined from Eqs. (14)-(16). Finally, the coefficients c_n in the temperature distribution given by Eq. (12) can be determined from the initial condition using quasi-orthogonality of the eigenfunctions, i.e.,

$$c_n = \frac{1}{N_n}\sum_{m=1}^{M}\frac{\bar{k}_m}{\bar{\alpha}_m}\int_{\gamma_{m-1}}^{\gamma_m}\theta_{0,m}(\xi)[A_{m,n}\cos(\omega_{m,n}\xi) + B_{m,n}\sin(\omega_{m,n}\xi)]d\xi \tag{18}$$

where the norm N_n is given by

$$N_n = \sum_{m=1}^{M}\frac{\bar{k}_m}{\bar{\alpha}_m}\int_{\gamma_{m-1}}^{\gamma_m}[A_{m,n}\cos(\omega_{m,n}\xi) + B_{m,n}\sin(\omega_{m,n}\xi)]^2 d\xi \tag{19}$$

Note that the key difference between the approach outlined above and the standard procedure for the case of no heat generation ($\bar{\beta}_m = 0$) [1,2] is that in this case, the spatial and temporal eigenvalues are related to each other through Eq. (12). This relationship is, in part, responsible for imaginary eigenvalues to exist in this problem. Further, it can be shown that the usual orthogonality relationship for multi-layer diffusion [1,2] applies for this problem, with no impact due to the source terms.

In general, the existence of imaginary eigenvalues must be evaluated by examining the roots of the determinant of Eqs. (14)-(17). For a general, M-layer body, it is difficult to express the determinant explicitly. Several aspects related to the existence of imaginary eigenvalues for both positive and negative $\bar{\beta}_m$ are examined in the next section for a special case of a two-layer body. The subsequent impact of imaginary eigenvalues on the computed temperature distribution is discussed in Section 4.

3. Special Case – two-layer one-dimensional body

A special case of a two-layer one-dimensional body with linear, temperature-dependent heat generation/consumption in both layers is considered. Such two-layer problems occur in several engineering applications. For example, the species diffusion problem encountered in a Li-ion half cell [20,24] involves generation/consumption term in the electrode layer due to charge/discharge processes. Thermal transport in a stack of closely-packed Li-ion cells can also be modeled by this problem. In this problem, heat removal from the boundaries is represented by Bi_A and Bi_B, while temperature-dependent heat generation/consumption within the layers is represented by $\bar{\beta}_1$ and $\bar{\beta}_2$. These are the key dimensionless parameters of the problem, in addition to property ratios $\bar{k}_1$ and $\bar{\alpha}_1$, and the geometrical ratio γ_1.

For simplicity, the same cooling conditions are assumed to exist on both ends, i.e., Bi_A=Bi_B=Bi. Note that $\bar{k}_2 = \bar{\alpha}_2 = 1$ by definition.

For a two-layer body under conditions stated above, the eigenvalues λ_n are given by roots of the determinant of Eqs. (14)-(17), which can be simplified to

$$f\left(\lambda^2\right) = \bar{k}_1\omega_1 \frac{-\bar{k}_1\omega_1 \sin\omega_1\gamma_1 + Bi\cos\omega_1\gamma_1}{\bar{k}_1\omega_1\cos\omega_1\gamma_1 + Bi\sin\omega_1\gamma_1} + \omega_2 \frac{-\omega_2\sin\left(\omega_2(1-\gamma_1)\right) + Bi\cos\left(\omega_2(1-\gamma_1)\right)}{\omega_2\cos\left(\omega_2(1-\gamma_1)\right) + Bi\sin\left(\omega_2(1-\gamma_1)\right)} = 0 \tag{20}$$

Where ω_1 and ω_2 are given by Eq. (13).

3.1. Imaginary λ_1 at large values of $\bar{\beta}_m$

While eigenequations for most thermal conduction problems admit only real roots, it is shown here that an imaginary value of λ may also satisfy Eq. (20). The existence of an imaginary root for λ is important, because it leads to exponentially increasing temperature, as predicted by Eq. (12).

In order to determine if Eq. (20) admits an imaginary root, and if so, determine that root, $\hat{\lambda}^2 = -\lambda^2$ is substituted in Eq. (20). With some algebraic simplification, one may obtain

$$f\left(\hat{\lambda}^2\right) = \bar{k}_1\hat{\omega}_1 \frac{\bar{k}_1\hat{\omega}_1 + Bi\coth\hat{\omega}_1\gamma_1}{\bar{k}_1\hat{\omega}_1\coth\hat{\omega}_1\gamma_1 + Bi} + \hat{\omega}_2 \frac{\hat{\omega}_2 + Bi\coth\left(\hat{\omega}_2(1-\gamma_1)\right)}{\hat{\omega}_2\coth\left(\hat{\omega}_2(1-\gamma_1)\right) + Bi} = 0 \tag{21}$$

where, $\hat{\omega}_m = \sqrt{\frac{\hat{\lambda}^2 - \bar{\beta}_m}{\bar{\alpha}_m}} = i\omega_m$ for m=1,2. Note that $i = \sqrt{-1}$ is the unit imaginary number. Eq. (21) may be interpreted as the eigenequation for imaginary eigenvalues of the two-layer problem, if one exists.

Appendix A shows that $f(\hat{\lambda}_n^2)$ is a monotonically increasing function for positive values of $\hat{\lambda}^2$, and therefore, imaginary values of λ. Therefore, a requirement for this equation to admit a root is that the function $f(\hat{\lambda}^2)$ must be less than zero at $\hat{\lambda}^2 = 0$. In addition, due to the monotonically increasing nature of f, there will be, at most, one imaginary root. Therefore, a condition for an imaginary root to exist can be derived by substituting $\hat{\lambda}^2 = 0$ in Eq. (21), resulting in

$$\bar{k}_1 \frac{-\bar{\beta}_1/\bar{\alpha}_1\bar{k}_1 + Bi\sqrt{\bar{\beta}_1/\bar{\alpha}_1}\cot\left(\sqrt{\bar{\beta}_1/\bar{\alpha}_1}\gamma_1\right)}{\bar{k}_1\sqrt{\bar{\beta}_1/\bar{\alpha}_1}\cot\left(\sqrt{\bar{\beta}_1/\bar{\alpha}_1}\gamma_1\right) + Bi} + \frac{-\bar{\beta}_2 + Bi\sqrt{\bar{\beta}_2}\cot\left(\sqrt{\bar{\beta}_2}(1-\gamma_1)\right)}{\sqrt{\bar{\beta}_2}\cot\left(\sqrt{\bar{\beta}_2}(1-\gamma_1)\right) + Bi} < 0 \tag{22}$$

For given values of Bi and geometrical and property parameters $\bar{k}_1$, $\bar{\alpha}_1$ and γ_1, Eq. (22) represents a condition on the heat generation coefficients $\bar{\beta}_1$ and $\bar{\beta}_2$ in order for an imaginary eigenvalue λ_1 to exist. Eq. (22) may be interpreted as a balance between heat generation/consumption in each layer ($\bar{\beta}_1$ and $\bar{\beta}_2$) and heat removal from the boundaries (Bi), for a given set of properties and relative thicknesses of the two layers.

As an illustration, Fig. 2(a) and 2(b) plot $f(\lambda^2)$ for a representative problem with $\bar{k}_1 = 0.5$, $\bar{\alpha}_1 = 2.0$, $\gamma_1 = 0.667$, $\bar{\beta}_1 = 0$, Bi = 10 over the ranges $-10 < \lambda^2 < 0$ and $0 < \lambda^2 < 120$ respectively, corresponding to imaginary and real values of λ, respectively. In both cases, curves are plotted for two different values of $\bar{\beta}_2$. Plots in the imaginary and real ranges of λ are shown separately in Fig. 2(a) and 2(b) due to the difference in scaling of the two plots. The x axis is denoted by a dotted line. These plots show that for real λ, i.e. $\lambda^2 > 0$, the eigenfunction is non-monotonic and admits an infinite number of real roots, as is usual for eigenvalue problems in thermal conduction. On the other hand, Fig. 2(a) shows that f is monotonic when $\lambda^2 < 0$, which indicates that in addition to the infinite number of real roots, one imaginary root may also exist. Since f increases with decreasing λ^2, therefore, one – and only one – imaginary root exists if f is negative at $\lambda^2 = 0$. This is indeed the case for the $\bar{\beta}_2 = 18$ curve, but not the $\bar{\beta}_2 = 12$ curve plotted in Fig. 2(a). Consequently, one imaginary root is found to exist for $\bar{\beta}_2 = 18$ and none for $\bar{\beta}_2 = 12$, as shown in Fig. 2(a). Physically, this means that convective cooling at the boundary is sufficient to prevent thermal runaway $\bar{\beta}_2 = 12$ at but at $\bar{\beta}_2 = 18$, the internal heating overwhelms boundary cooling, resulting in imaginary eigenvalue, and therefore, exponentially increasing temperature. On the other hand, both cases considered here admit an infinite number of real roots, some of which can be seen in Fig. 2(b).

Fig. 3 plots the magnitude of the imaginary root, λ_1, as a function of $\bar{\beta}_2$ for three different values of Bi. Other problem parameters are $\bar{k}_1 = 0.5; \bar{\alpha}_1 = 2.0;\ \gamma_1 = 0.667; \bar{\beta}_1 = -5$. Fig. 3 shows that the magnitude of λ_1 increases rapidly at first, and then linearly, with increasing $\bar{\beta}_2$. Note that $\bar{\beta}_2$ represents how rapidly heat generation rate increases with temperature. The higher the value of $\bar{\beta}_2$, the more aggressive is the heating, and therefore, it is expected that the magnitude of the imaginary eigenvalue will increase with $\bar{\beta}_2$. The greater the value of λ_1, the greater is the divergence in temperature at large times, as seen in the exponential term in Eq. (12). For each Bi plotted in Fig. 3, there is a threshold value of $\bar{\beta}_2$, below which, there is no imaginary eigenvalue. This is because $\bar{\beta}_1$ is negative, and therefore, the system is able to withstand a small positive value of $\bar{\beta}_2$ without divergence at large times. As expected, the greater the value of Bi, representing heat removal from the boundaries, the greater is this threshold value of $\bar{\beta}_2$.

A physical interpretation of the existence of an imaginary eigenvalue is that it results in exponentially increasing temperature with time by changing the sign within the exponential transient term in Eq. (12). This occurs because of the positive relationship between heat generation rate and temperature. As temperature increases, heat generation rate also increases, which further increases the temperature. Beyond a certain limit, the boundary is unable to remove sufficient heat to keep the increasing temperature in check, resulting in thermal runaway, which is a serious concern for the safety of Li-ion cells [22,25]. It is of much interest to proactively predict the onset of such thermal runaway. In this case, Eq. (22) represents a limit on the heat generation coefficients in the two layers such that an exponentially growing temperature is averted. It is clear that when $\bar{\beta}_1$ and $\bar{\beta}_2$ are both negative, Eq. (22) is not satisfied under any conditions. As a result, there is no imaginary eigenvalue, and therefore, the temperature distribution is not expected to diverge. This is expected because negative $\bar{\beta}_1$ and $\bar{\beta}_2$ result in damping of the heat generation rate. On the other hand, when one or both of $\bar{\beta}_1$ and $\bar{\beta}_2$ are positive, then an imaginary root may exist if $\bar{\beta}_1$ and $\bar{\beta}_2$ satisfy Eq. (22).

Several special cases of Eq. (22) are of interest. The condition for imaginary λ_1 in case of isothermal boundaries may be obtained by setting $Bi \to \infty$ in Eq. (22), which results in

$$\bar{k}_1\sqrt{\bar{\beta}_1/\bar{\alpha}_1}\cot\left(\sqrt{\bar{\beta}_1/\bar{\alpha}_1}\gamma_1\right) + \sqrt{\bar{\beta}_2}\cot\left(\sqrt{\bar{\beta}_2}(1-\gamma_1)\right) < 0 \tag{23}$$

The isothermal boundary condition results in greatest-possible heat removal from the boundaries, and therefore, it is expected that the condition for divergence will be more relaxed, i.e., divergence will occur at greater values of $\bar{\beta}_1$ and $\bar{\beta}_2$ than with a finite value of Bi.

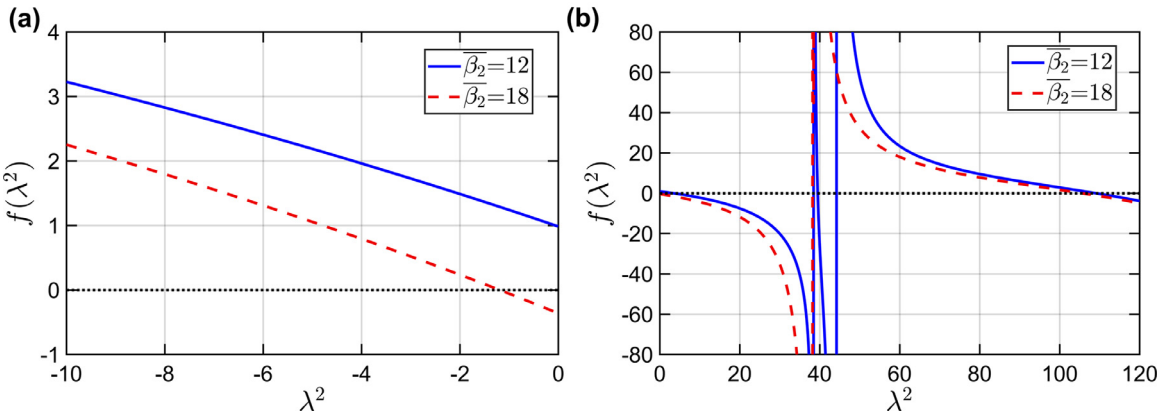

Fig. 2. Plot of the eigenequation for the two-layer problem (Eq. (21)) for (a) imaginary and (b) real values of λ. Two cases with $\bar{\beta}_2 = 12$ and $\bar{\beta}_2 = 18$ are shown. Other parameter values are $\bar{k}_1 = 0.5; \bar{\alpha}_1 = 2.0;\ \gamma_1 = 0.667; Bi = 10;\ \bar{\beta}_1 = 0$. Note that there are infinite real eigenvalues in each case, but zero or one imaginary eigenvalue for the two cases, respectively.

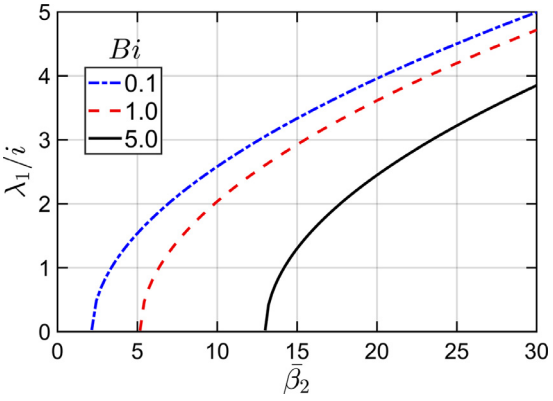

Fig. 3. Plot of the magnitude of the imaginary eigenvalue for a two-layer problem as a function of $\bar{\beta}_2$ for three different values of Bi. Other parameter values are $\bar{k}_1 = 0.5; \bar{\alpha}_1 = 2.0;\ \gamma_1 = 0.667; \bar{\beta}_1 = -5$.

On the other extreme, heavily insulated boundaries (Bi → 0) do not permit any heat removal, and therefore, divergence of the temperature distribution may be expected when $\bar{\beta}_1$ and $\bar{\beta}_2$ are both positive. A condition of divergence for very small Bi can be obtained by setting Bi → 0 in the general condition given by Eq. (22). This results in

$$-\bar{k}_1\sqrt{\frac{\bar{\beta}_1}{\bar{\alpha}_1}}\tan\left(\sqrt{\frac{\bar{\beta}_1}{\bar{\alpha}_1}}\gamma_1\right) - \sqrt{\bar{\beta}_2}\tan\left(\sqrt{\bar{\beta}_2}(1-\gamma_1)\right) < 0 \qquad (24)$$

It can be easily shown that Eq. (24) is satisfied when $\bar{\beta}_1$ and $\bar{\beta}_2$ are both positive. This is indeed the worst-possible case in terms of avoiding thermal runaway, because even a small positive feedback between temperature and heat generation is bound to result in divergence in temperature with time since no heat is allowed to escape.

As another special case, the two-layer relationships above can be reduced to a single-layer body by setting $\bar{k}_1 = \bar{\alpha}_1 = 1$, $\gamma_1 = 0.5$ and $\bar{\beta}_1 = \bar{\beta}_2 = \bar{\beta}$ in Eq. (22). This substitution, followed by mathematical rearrangement results in the following expression for the limiting value of $\bar{\beta}$ for a single-layer body

$$\frac{-\bar{\beta} + Bi\sqrt{\bar{\beta}}\cot\left(\sqrt{\bar{\beta}/2}\right)}{\sqrt{\bar{\beta}}\cot\left(\sqrt{\bar{\beta}/2}\right) + Bi} = 0 \qquad (25)$$

which implies that in order for an imaginary eigenvalue to exist, and therefore, divergence at large times, $\bar{\beta}$ must equal the first root of the equation $x\tan x - \frac{Bi}{2} = 0$, which is indeed the Cartesian equivalent of the condition derived in a past paper for divergence in a single-layer cylindrical body [22]. This shows that the results presented here correctly reduce to the previously-presented result for the special case of a single-layer body. Similar treatment of Eq. (23) for isothermal boundaries shows that the single-layer limiting condition for $\bar{\beta}$ is $\bar{\beta} = \pi^2$.

As an illustration of the limits on various problem parameters for keeping the temperature field within bounds at large times, Fig. 4 identifies regions in the $\bar{\beta}_1 - \bar{\beta}_2$ space in which the temperature is bounded or not, based on the existence of the imaginary eigenvalue λ_1. Plots are presented for two different values of Bi, and other problem parameters are $\bar{k}_1 = 0.5$, $\gamma_1 = 0.667$ and $\bar{\alpha}_1 = 2.0$. Fig. 4 shows that temperature remains bounded when both $\bar{\beta}_1$ and $\bar{\beta}_2$ are negative, which is expected because negative values result in heat absorption, and therefore, damping of the temperature field over time. In fact, in such a case, the temperature field is expected to decay to zero at large times. On the other hand, when both $\bar{\beta}_1$ and $\bar{\beta}_2$ are positive, the two must both be reasonably small in magnitude in order for the temperature to not diverge. Further, a large positive value of either $\bar{\beta}_1$ or $\bar{\beta}_2$ is tolerable, provided that the other parameter is sufficiently negative. This corresponds to consumption in one layer counteracting generation in the other in order to keep the temperature distribution bounded. If one of the parameters is positive and too large, it is nearly impossible to keep temperature within bounds because it requires the other parameter to be negative and extremely large in magnitude. Fig. 4(a) and 4(b) also illustrate the impact of Bi on these characteristics. As Bi increases, the capability of the system to sustain generation improves due to greater heat removal from the boundaries. This is the reason why the converge region is larger at Bi=1.5 (Fig. 4(b)) than at Bi=0.5 (Fig. 4(a)), particularly in the first quadrant.

In practical applications, it is often of interest to predict the maximum tolerable source coefficient before thermal runaway occurs. Since this limit is a function of the cooling co+nditions, Fig. 5 presents a plot of maximum value of $\bar{\beta}_2$ to ensure converged temperature as a function of Bi. Other parameter values are $\bar{k}_1 = 0.5, \bar{\alpha}_1 = 2.0,\ \gamma_1 = 0.667,\ \bar{\beta}_1 = 0.5$. Based on Eq. (22), it is found that for small values of Bi, $\bar{\beta}_{2max}$ is small and nearly invariant of Bi. As cooling conditions improve, the system is able to tolerate greater and greater values of the source coefficient in the second layer. Eventually, this effect saturates as Bi increases and the boundary condition becomes closer and closer to isothermal. In this regime, $\bar{\beta}_{2max}$ approaches the isothermal limit given by Eq. (23), also shown in Fig. 5 as a dashed line. Note that for

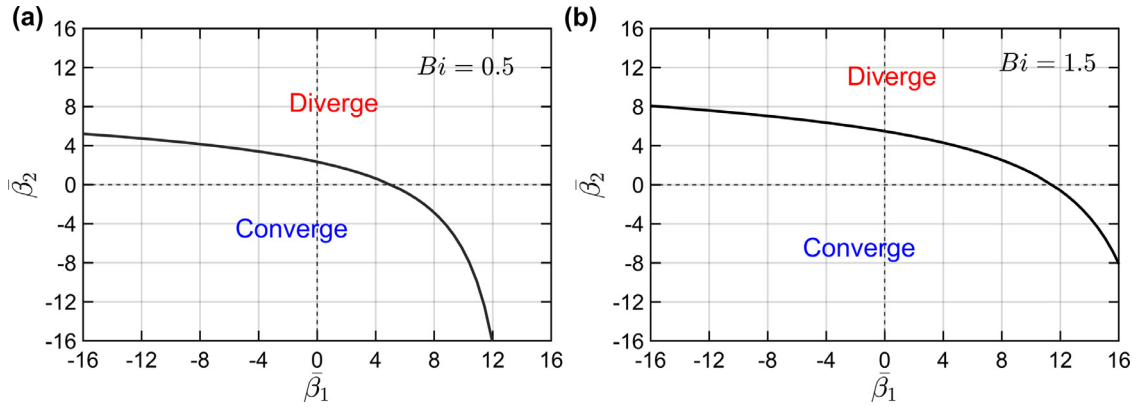

Fig. 4. Colormap showing regimes in the $\bar{\beta}_1 - \bar{\beta}_2$ space in which temperature at large times converges or diverges. Both negative and positive values of $\bar{\beta}_1$ and $\bar{\beta}_2$ are plotted. Other problem parameters are $\bar{k}_1 = 0.5; \bar{\alpha}_1 = 2.0;\ \gamma_1 = 0.667$. Plots are presented for (a) $Bi = 0.5$ and (b) $Bi = 1.5$.

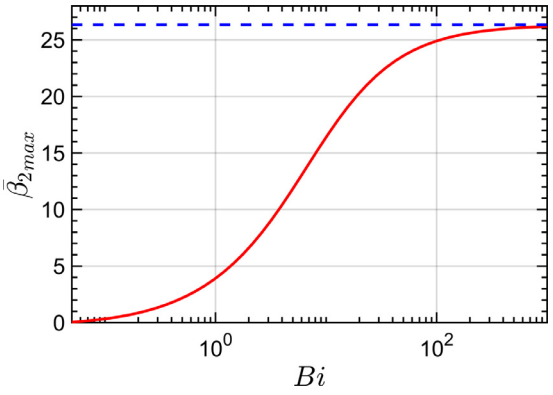

Fig. 5. Maximum tolerable value of $\bar{\beta}_2$ to avoid divergence in temperature field at large times as a function of *Bi*. Other parameter values are $\bar{k}_1 = 0.5; \bar{\alpha}_1 = 2.0;\ \gamma_1 = 0.667;\ \bar{\beta}_1 = 0.5$. For Bi values lower than plotted, no positive value of $\bar{\beta}_2$ is tolerable due to the presence of a positive $\bar{\beta}_1$. The dashed line shows the isothermal limit obtained from Eq. (23).

Bi smaller than plotted in Fig. 5, no positive value of $\bar{\beta}_2$ ensures converged temperature, because when Bi is small, even if $\bar{\beta}_2$ is as small as 0, there is still divergence due to the positive value of $\bar{\beta}_1$ due to insufficient heat removal from the boundaries.

3.2. *Imaginary* $\omega_{m,n}$ *at large negative values of* $\bar{\beta}_m$

The discussion above shows that imaginary eigenvalues for λ_1 may exist for large positive values of $\bar{\beta}_1$ or $\bar{\beta}_2$. In addition, Eq. (13) indicates that imaginary values of spatial eigenvalues $\omega_{m,n}$ may occur when $\bar{\beta}_m$ is negative and large in magnitude, even when λ_n is real. Unlike the λ_1 case considered in section 3.1, an imaginary value of $\omega_{m,n}$ does not result in divergence in temperature at large times because it does not cause any change in the sign of the term within the exponential transient term in Eq. (12). A condition for such imaginary eigenvalues to occur in any layer is simply that $\bar{\beta}_m$ must be negative and of a magnitude greater than the square of the first real root of the eigenequation given by Eq. (20). An explicit expression for the real roots of the eigenequation is not available for the present problem, as is the case for several thermal conduction problems [1,2]. The eigenvalues are determined numerically by identifying intervals where the function f changes signs over the interval, and then carrying out successive Newton-Raphson iterations in that interval to compute the root. Accuracy of the numerical approach is verified by ensuring accurate determination of roots of functions with well-known roots.

Sections 3.1 and 3.2 illustrate the existence of two distinct types of imaginary eigenvalues in this problem when the heating coefficients $\bar{\beta}_m$ are of large magnitude, either positive or negative. In order to illustrate when such imaginary eigenvalues occur, a two-layer problem with generation/consumption only in the second layer is considered. For this problem, Fig. 6 presents a plot showing regions in the $\bar{\beta}_2 - \mathrm{Bi}$ space where either $\omega_{2,1}$ is imaginary, based on Eq. (13), or λ_1 is imaginary, based on Eq. (21). These two types of imaginary eigenvalues occur for large magnitudes of $\bar{\beta}_2$ when negative or positive, respectively. Other problem parameters are $\bar{\beta}_1 = 0$, $\bar{k}_1 = 0.5$, $\gamma_1 = 0.667$. Fig. 6(a) and 6(b) present plots for $\bar{\alpha}_1 = 2.0$, and $\bar{\alpha}_1 = 1.0$, respectively. For a given value of Bi, $\omega_{2,1}$ is imaginary for low values of $\bar{\beta}_2$. As $\bar{\beta}_2$ increases, there is a region where all eigenvalues are real. Once the heating coefficient becomes positive and exceeds a threshold, λ_1 becomes imaginary. The larger the value of Bi, corresponding to more effective cooling at the boundaries, the greater is the threshold magnitude of $\bar{\beta}_2$ in order to result in imaginary $\omega_{2,1}$. On the other hand, at higher values of Bi, the upper threshold for $\bar{\beta}_2$ in order to result in imaginary λ_1 increases. This is because more effective cooling at the boundary moves the system away from divergence, thus requiring a larger value of $\bar{\beta}_2$ to result in an imaginary value of λ_1. These characteristics partly depend on other parameters as well. For example, with a lower value of $\bar{\alpha}_1 = 1.0$, corresponding to more effective thermal diffusion in the heat-generating second layer, Fig. 6(b) shows a much flatter threshold for imaginary $\omega_{2,1}$. This indicates a lower tolerance for negative values of $\bar{\beta}_2$ before $\omega_{2,1}$ turns imaginary. On the other hand, the threshold for imaginary λ_1 remains largely independent of $\bar{\alpha}_1$.

Note that the theoretical results derived in Sections 2 and 3 are valid for diffusion-based, continuum heat/mass transfer. Subcontinuum effects occurring in bodies of very small lengthscales and/or over very short timescales are not accounted for in this work.

4. Impact of Imaginary Eigenvalues on Temperature Solution

The previous section showed that eigenvalues in one or more layers may become imaginary if $\bar{\beta}_m$ is sufficiently large in magnitude, whether positive or negative. It is of interest to determine if the existence of imaginary eigenvalues, for example, as shown in Fig. 6, may impact the computation of temperature distribution in a multilayer body. While past work has emphasized the importance of accounting for imaginary eigenvalues in 2D and 3D multilayer problems, a formal proof that temperature remains real despite imaginary eigenvalues – an important practical matter – is missing. This section investigates the impact of imaginary eigen-

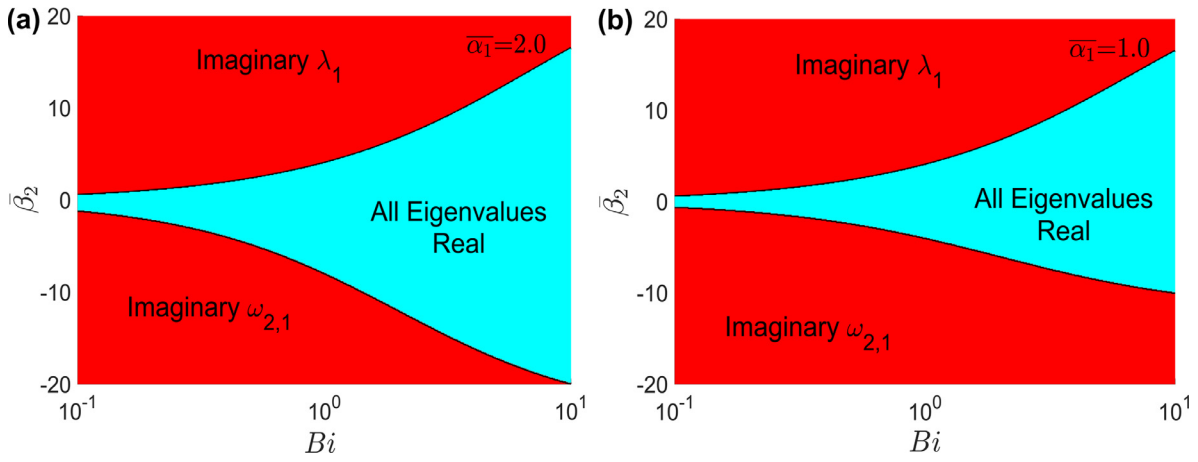

Fig. 6. Colormap showing regimes in the $Bi - \bar{\beta}_2$ space where $\omega_{2,1}$ or λ_0 may be real or imaginary. (a) $\bar{\alpha}_1 = 2.0$; (b) $\bar{\alpha}_1 = 0.5$. Other problem parameters are $\bar{k}_1 = 0.5$; $\gamma_1 = 0.667$, $\bar{\beta}_1$=0.

values on the predicted temperature distribution, and proves that despite any imaginary eigenvalues that may exist, the predicted temperature distribution, given by Eq. (12) remains real.

Firstly, it is clear that the temperature distribution remains real for an imaginary value of λ_1, because the exponential term in Eq. (12) includes $-\lambda_1^2$. Therefore, while an imaginary value of λ_1 causes exponentially growing temperature, it does not cause temperature to become imaginary.

On the other hand, the impact of $\omega_{m,n}$ turning imaginary on the temperature distribution is more difficult to observe, since $\omega_{m,n}$ appears in multiple terms inside the spatial term in Eq. (12), including implicitly in the coefficients. In order to prove that temperature distribution remains real even when $\omega_{m,n}$ may be imaginary, it is important to first note that based on Eq. (13), $\omega_{m,n}$, if imaginary, will be purely imaginary. Further, the cosine and sine of a purely imaginary number is purely real and purely imaginary, respectively. Therefore, referring to Eq. (12), in order to prove that the temperature distribution remains purely real for any layer, it is sufficient to prove that the following two statements are correct for each layer, m=1,2…M:

Statement A: If $\omega_{m,n}$ is purely imaginary, then $A_{m,n}$ is purely real and $B_{m,n}$ is purely imaginary.

Statement B: If $\omega_{m,n}$ is purely real, then $A_{m,n}$ is purely real and $B_{m,n}$ is purely real.

Statements A and B are proved recursively, i.e., assuming that Statements A and B are true for m=m*, it is proved that Statements A and B are also true for m=m*+1. Further, it is proved that Statements A and B are true for m=1, thereby proving Statements A and B for each layer.

Based on the interfaces conditions given by Eq. (16) and (17), the coefficients $A_{m^*+1,n}$ and $B_{m^*+1,n}$ can be written in terms of $A_{m*,n}$ and $B_{m*,n}$ as follows:

$$A_{m^*+1,n} = p_{m^*} A_{m^*,n} + q_{m^*} B_{m^*,n} \tag{26}$$

$$B_{m^*+1,n} = r_{m^*} A_{m*,n} + s_{m^*} B_{m^*,n} \tag{27}$$

where

$$p_{m^*} = \left[\cos\omega_{m^*,n}\gamma_{m^*} \cos\omega_{m^*+1,n}\gamma_{m^*} + \frac{\bar{k}_{m^*}\omega_{m^*,n}}{\bar{k}_{m^*+1}\omega_{m+1,n}} \sin\omega_{m^*+1,n}\gamma_{m^*} \sin\omega_{m^*,n}\gamma_{m^*} \right] \tag{28}$$

$$q_{m^*} = \left[\sin\omega_{m^*,n}\gamma_{m^*} \cos\omega_{m^*+1,n}\gamma_{m^*} - \frac{\bar{k}_{m^*}\omega_{m^*,n}}{\bar{k}_{m^*+1}\omega_{m^*+1,n}} \sin\omega_{m^*+1,n}\gamma_{m^*} \cos\omega_{m^*,n}\gamma_{m^*} \right] \tag{29}$$

$$r_{m^*} = \left[\cos\omega_{m^*,n}\gamma_{m^*} \sin\omega_{m^*+1,n}\gamma_{m^*} - \frac{\bar{k}_{m^*}\omega_{m^*,n}}{\bar{k}_{m^*+1}\omega_{m^*+1,n}} \sin\omega_{m^*,n}\gamma_{m^*} \cos\omega_{m^*+1,n}\gamma_{m^*} \right] \tag{30}$$

$$s_{m^*} = \left[\sin\omega_{m^*,n}\gamma_{m^*} \sin\omega_{m^*+1,n}\gamma_{m^*} + \frac{\bar{k}_{m^*}\omega_{m^*,n}}{\bar{k}_{m^*+1}\omega_{m^*+1,n}} \cos\omega_{m^*,n}\gamma_{m^*} \cos\omega_{m^*+1,n}\gamma_{m^*} \right] \tag{31}$$

Now, when $\omega_{m^*,n}$ is purely imaginary (Statement A), $\omega_{m^*+1,n}$ may be either purely real or purely imaginary. In the former case, p_{m^*} and r_{m^*} are both purely real, while q_{m^*} and s_{m^*} are both purely imaginary. Since $A_{m^*,n}$ and $B_{m^*,n}$ are purely real and purely imaginary, respectively, under Statement A, it follows from Eq. (26) and (27) that $A_{m^*+1,n}$ and $B_{m^*+1,n}$ are both purely real. On the other hand, when $\omega_{m^*+1,n}$ is purely imaginary, p_{m^*} and s_{m^*} are both purely real, while q_{m^*} and r_{m^*} are both purely imaginary. Therefore, it follows from Eq. (26) and (27) that $A_{m^*+1,n}$ and $B_{m^*+1,n}$ are both purely real and purely imaginary, respectively. These considerations prove that when Statement A is true for m=m*, it is true for m=m*+1 as well. A similar set of arguments prove that when Statement B is true for m=m*, it is true for m=m*+1 as well.

In order to complete the recursion-based proof, it must be proved that Statements A and B are true for m*=1. In this case, $A_{1,n}$ is always pure real since it is chosen to be equal to 1. From Eq. (14), $B_{1,n}$ is purely real when $\omega_{1,n}$ is purely real, and $B_{1,n}$ is purely imaginary when $\omega_{1,n}$ is purely imaginary. This proves Statements A and B for m=1. Therefore, Statements A and B are proved to be true for each layer through recursion.

Statements A and B, in turn, establish that, based on Eq. (12), regardless of whether the eigenvalues of a layer, $\omega_{m,n}$, are purely real or purely imaginary, the temperature distribution in that layer will always be real. When $\omega_{m,n}$ is real, all quantities within the square bracket in Eq. (12) are real. When $\omega_{m,n}$ is purely imaginary, the two terms in the first product in the square bracket ($A_{m,n}$ and $\cos\omega_{m,n}\xi$) in Eq. (12) are both real, while the two terms in the second product ($B_{m,n}$ and $\sin\omega_{m,n}\xi$) are both purely imaginary, leading to an overall purely real temperature.

While it is clearly expected that the temperature distribution in a well-defined problem must be real, the discussion above provides a formal mathematical proof even for a scenario where some eignevalues may be imaginary.

Since the temperature distribution based on Eq. (12) remains purely real regardless of whether some or all of the eigenvalues are imaginary, therefore, it is important when computing the temperature to include all eigenvalues, whether real or imaginary. Ignoring imaginary eigenvalues is likely to result in inaccurate temperature prediction. To illustrate this, Fig. 7(a) and 7(b) plot temperature distributions at multiple times when either all eigenvalues – real and imaginary – are considered, or when imaginary eigenvalues are ignored. For comparison, results from a finite-difference

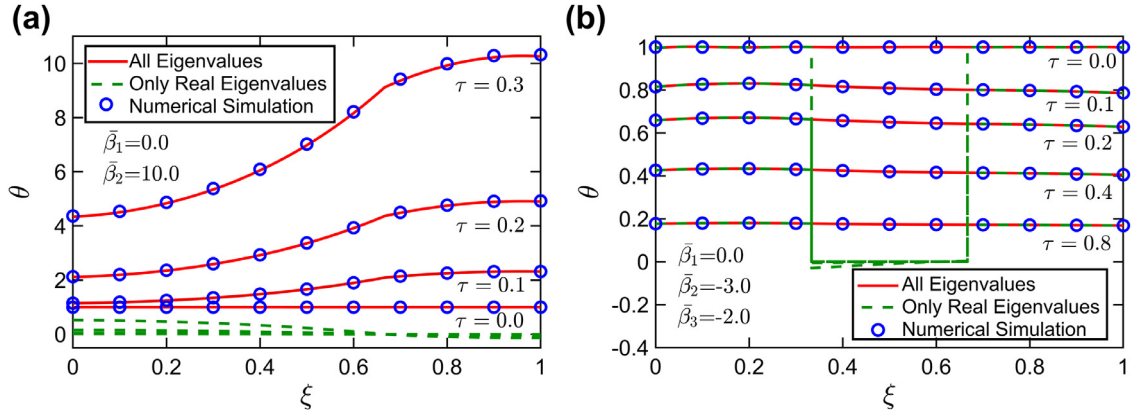

Fig. 7. Importance of accounting for all imaginary eigenvalues: Temperature distribution in the multi-layer body at different times starting with an initial uniform temperature $\theta_{0,m} = 1$. (a) Two-layer body with $\bar{k}_1 = 0.5$; $\bar{\alpha}_1 = 2.0$; $\gamma_1 = 0.667$; $Bi = 0.1$; $\bar{\beta}_1 = 0$, $\bar{\beta}_2 = 10$; (b) Three-layer body with $\bar{k}_1 = 0.5$, $\bar{k}_2 = 0.6$, $\bar{\alpha}_1 = 2.0$, $\bar{\alpha}_1 = 3.0$, $\gamma_1 = 0.333$, $\gamma_2 = 0.667$, Bi=0.1, $\bar{\beta}_1 = 0$, $\bar{\beta}_2 = -3$, $\bar{\beta}_3 = -2$. In each case, temperature distribution is computed by ignoring or keeping all imaginary eigenvalues. For comparison, results from a finite-element simulation are also plotted.

numerical simulation are also plotted. The numerical simulation is carried out using a fully implicit finite difference method. Each layer is divided into 500 elements and the simulation time is also divided into 1000 timesteps. One node is assigned to the interface to facilitate the conservation of temperature and flux. Fig. 7(a) considers a two-layer body with $\bar{k}_1 = 0.5$, $\bar{\alpha}_1 = 2.0$, $\gamma_1 = 0.667$, Bi=0.1, $\bar{\beta}_1 = 0$, $\bar{\beta}_2 = 10$, $\theta_{0,m} = 1$, for m=1,2. In this case, temperature diverges at large times due to the large, positive value of $\bar{\beta}_2$. In contrast, Fig. 7(b) considers a three-layer body with $\bar{k}_1 = 0.5$, $\bar{k}_2 = 0.6$, $\bar{\alpha}_1 = 2.0$, $\bar{\alpha}_2 = 3.0$, $\gamma_1 = 0.333$, $\gamma_2 = 0.667$, Bi=0.1, $\bar{\beta}_1 = 0$, $\bar{\beta}_2 = -3$, $\bar{\beta}_3 = -2$, $\theta_{0,m} = 1$ for m=1,2,3. In this case, no value of $\bar{\beta}_m$ is positive, and therefore, the temperature distribution is not expected to diverge at large times. Fig. 7(a) and 7(b) show that ignoring imaginary eigenvalues results in a completely inaccurate temperature distribution in both cases. On the other hand, when all real and imaginary eigenvalues are accounted for, the predicted temperature distribution is correct and in good agreement with finite-difference simulation results. In the case of diverging temperature, ignoring the imaginary eigenvalue leads to a completely inaccurate prediction. Even when there is no divergence, ignoring imaginary eigenvalues still causes error. Note that accounting for imaginary eigenvalues is particularly important because in the present problem, imaginary eigenvalues, if present, are the first few, which are known to contribute the most to the infinite series in which temperature has been expressed.

5. Temperature Computation for a Practical Problem

The theoretical methodology discussed in this paper is used for computing temperature distribution for a practical problem. A stack of two identical, prismatic Li-ion cells is considered. Abuse conditions such as high temperature, nail penetration or overcharging can lead to initiation of exothermic decomposition reactions [4]. As temperature increases, so does the rate of such reactions, due to which, heat generation rate also increases. While this dependence is governed by non-linear Arrhenius kinetics [26], it is often modeled as a linear relationship as a first-order approximation [22,23]. It is assumed that the first cell in the stack undergoes such temperature-dependent heat generation. Heat transfer is assumed to be one-dimensional, justified by the thin nature of the cells compared to lateral dimensions. No internal heat generation occurs in the second cell. The two ends of the two-layer body are assumed to be convectively cooled with Bi=0.1. For this problem, temperature distribution is computed and plotted in Fig. 8 for two different values of the source coefficient in the first cell, $\overline{\beta}_1 = 0.1$ and $\overline{\beta}_1 = 2.0$, which represent mild and aggressive exothermic reactions, respectively. Fig. 8 plots temperature distributions within the two-cell stack at different times for these two different cases. Since Li-ion cells vary significantly in size and thermal properties, the results are presented in non-dimensional form for generality. Fig. 8 shows that when $\overline{\beta}_1$ is reasonably small, i.e., heat generation rate increases rather slowly with temperature, the cell temperature does not diverge at large time, because the convective boundary condition is able to dissipate the heat generated and prevent thermal runaway. On the other hand, when $\overline{\beta}_1$ is larger, corresponding to a rapid rise in heat generation rate with increasing temperature, the convective cooling at the boundary is no longer able to keep up with the positive feedback between temperature and heat generation, resulting in exponentially growing temperature. In addition to the cell being abused, the cell with no internal heat generation also experiences very large temperature due to the large amount of heat being generated in its neighbor. This observation indeed corresponds to the phenomenon of thermal runaway propagation in a Li-ion cell [4,23], where heat generated in exothermic reactions increases temperature, which in turn increases the rates of such reactions, resulting in thermal runaway and catastrophic failure of the Li-ion cell. The mathematical model developed in this work is able to model such a phenomena in practical, multi-layer systems, and contribute towards a capability for proactive prediction of thermal runaway.

6. Conclusions

Thermal conduction in a multilayer body is a well-researched class of problems with several applications in engineering systems. This paper analyzes imaginary eigenvalues that appear in an important thermal conduction problem involving linear, temperature-dependent heat generation in a multi-layer one-dimensional body. It is shown that two distinct types of imaginary eigenvalues may appear in such a problem. The first type may be interpreted as leading to exponentially rising temperature due to change in sign of the term within the transient exponent. Conditions for the appearance of imaginary eigenvalues are derived. Quite importantly, it is shown that despite imaginary eigenvalues, the computed temperature remains real, and therefore, imaginary eigenvalues must not be discarded.

In addition to advancing the fundamental understanding of multilayer heat and mass transfer, it is expected that this work has practical relevance for engineering applications such as thermal runaway in Li-ion cells, where temperature-dependent heat

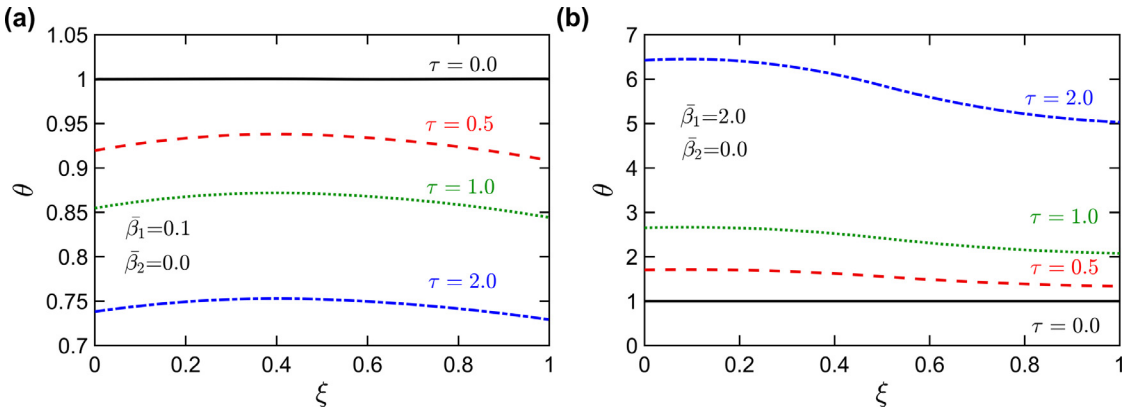

Fig. 8. Temperature computation for a practical application: Temperature distribution at multiple times for a stack of two Li-ion cells, with temperature-dependent exothermic decomposition reaction in one of the cells due to abuse. Plot for two distinct values of the source coefficient show two very different thermal outcomes of the cell.

generation results in catastrophic failure and explosion. The ability to predict the thermal fate of a closely-packed stack of cells based on the model developed here may be of much practical importance. The present work may also be applicable to other multilayer energy conversion/storage systems such as fuel cells and solar cells where linear, temperature/concentration-dependent generation may occur. In addition to heat transfer, the work described here is also relevant to mass transfer problems involving first-order chemical reactions resulting in generation/consumption of species in multiple layers. Such a scenario occurs, for example, in a Li-ion cell, where Li ion generation/consumption occurs in the electrode layers, along with no generation/consumption in the separator layer.

CRediT Authorship Contribution Statement

A. Jain – Conceptualization, Methodology, Formal Analysis, Validation, Investigation, Data Curation, Supervision, Project Administration; M. Parhizi – Conceptualization, Methodology, Validation, Data Curation; L. Zhou – Methodology, Validation, Data Curation; G. Krishnan – Conceptualization, Methodology, Validation, Data Curation. All authors contributed towards Writing Original Draft, Review and Editing.

Declaration of Competing Interest

None

Acknowledgments

This material is based upon work supported by CAREER Award No. CBET-1554183 from the National Science Foundation.

Appendix A: Proof that f defined by equation (21) is an increasing function

Consider the function f defined by Eq. (21) as

$$f\left(\hat{\lambda}^2\right) = f_1 + f_2 = \bar{k}_1\hat{\omega}_1 \frac{\bar{k}_1\hat{\omega}_1 + Bi\coth\hat{\omega}_1\gamma_1}{\bar{k}_1\hat{\omega}_1\coth\hat{\omega}_1\gamma_1 + Bi} + \hat{\omega}_2 \frac{\hat{\omega}_2 + Bi\coth\hat{\omega}_2(1-\gamma_1)}{\hat{\omega}_2\coth\hat{\omega}_1(1-\gamma_1) + Bi} \quad \text{(A1)}$$

where $\hat{\omega}_m = \sqrt{\frac{\hat{\lambda}^2 - \bar{\beta}_m}{\bar{\alpha}_m}}$, m=1,2.

Consider only the first term in Eq. (A1), denoted by f_1. Differentiating with respect to $\hat{\lambda}$, one may obtain

$$\frac{\partial f_1}{\partial}\hat{\lambda} = \frac{\bar{k}_1}{\bar{\alpha}_1}\hat{\lambda}\,\frac{\bar{k}_1\hat{\omega}_1\coth\hat{\omega}_1\gamma_1 + 2\bar{k}_1Bi + \bar{k}_1\gamma_1\hat{\omega}_1^2\mathrm{csch}^2\hat{\omega}_1\gamma_1 + Bi^2\left(\coth\hat{\omega}_1\gamma_1 - \hat{\omega}_1\gamma_1\mathrm{csch}^2\hat{\omega}_1\gamma_1\right)/\hat{\omega}_1}{\left[\bar{k}_1\hat{\omega}_1\coth\hat{\omega}_1\gamma_1 + Bi\right]^2} \quad \text{(A2)}$$

The first three terms in the numerator on the right hand side in Eq. (A2) are all positive. The third term can also be shown to be positive as follows:

$$\frac{\coth\hat{\omega}_1\gamma_1 - \hat{\omega}_1\gamma_1\mathrm{csch}^2\hat{\omega}_1\gamma_1}{\hat{\omega}_1} = \frac{e^{\hat{\omega}_1\gamma_1} + e^{-\hat{\omega}_1\gamma_1}}{e^{\hat{\omega}_1\gamma_1} - e^{-\hat{\omega}_1\gamma_1}} - \frac{4\hat{\omega}_1\gamma_1}{\left[e^{\hat{\omega}_1\gamma_1} - e^{-\hat{\omega}_1\gamma_1}\right]^2} = \frac{e^{2\hat{\omega}_1\gamma_1} - e^{-2\hat{\omega}_1\gamma_1} - 4\hat{\omega}_1\gamma_1}{\left[e^{\hat{\omega}_1\gamma_1} - e^{-\hat{\omega}_1\gamma_1}\right]^2\hat{\omega}_1} \quad \text{(A3)}$$

Using series expansion, one may simplify

$$\frac{\coth\hat{\omega}_1\gamma_1 - \hat{\omega}_1\gamma_1\mathrm{csch}^2\hat{\omega}_1\gamma_1}{\hat{\omega}_1} \quad \frac{\left[1 + 2\hat{\omega}_1\gamma_1 + \frac{(2\hat{\omega}_1\gamma_1)^2}{2} + \frac{(2\hat{\omega}_1\gamma_1)^3}{6} + \ldots\right] - \left[1 - 2\hat{\omega}_1\gamma_1 + \frac{(2\hat{\omega}_1\gamma_1)^2}{2} - \frac{(2\hat{\omega}_1\gamma_1)^3}{6} + \ldots\right] - 4\hat{\omega}_1\gamma_1}{\left[e^{\hat{\omega}_1\gamma_1} - e^{-\hat{\omega}_1\gamma_1}\right]^2\hat{\omega}_1} \quad \text{(A4)}$$

Resulting in

$$\frac{\coth\hat{\omega}_1\gamma_1 - \hat{\omega}_1\gamma_1\mathrm{csch}^2\hat{\omega}_1\gamma_1}{\hat{\omega}_1} = \frac{2\frac{(2\hat{\omega}_1\gamma_1)^3}{6\hat{\omega}_1} + 2\frac{(2\hat{\omega}_1\gamma_1)^5}{120\hat{\omega}_1} + \cdots}{\left[e^{\hat{\omega}_1\gamma_1} - e^{-\hat{\omega}_1\gamma_1}\right]^2} \quad \text{(A5)}$$

This shows that the numerator on the right hand side of Eq. (A2), and therefore, $\frac{\partial f_1}{\partial\hat{\lambda}}$ is positive for positive values of $\hat{\lambda}^2$. Similarly, one can show that $\frac{\partial f_2}{\partial\hat{\lambda}}$ is positive. This shows that f in Eq. (A1) is an increasing function. This, in turn, helps establish, in section 3.1, that a requirement for an imaginary eigenvalue to exist is that $f(0) < 0$

References

[1] D.W. Hahn, M.N. Özişik, Heat Conduction, Wiley, New York, 2012.
[2] M.D. Mikhailov, M.N. Özişik, Unified Analysis and Solutions of Heat and Mass Diffusion, Dover Publications, New York, 1994.
[3] F. de Monte, An analytic approach to the unsteady heat conduction processes in one-dimensional composite media, Int. J. Heat Mass Transfer 45 (2002) 1333–1343.
[4] T.M. Bandhauer, S. Garimella, T.F. Fuller, A critical review of thermal issues in Lithium-ion batteries,', J. Electrochem. Soc. 158 (2011) R1–R25.
[5] L. Choobineh, A. Jain, An explicit analytical model for rapid computation of temperature field in a three-dimensional integrated circuit, Int. J. Therm. Sci. 87 (2015) 103–109.
[6] H. French, Heat Transfer and Fluid Flow in Nuclear System (1981) 1st Ed.
[7] M. Cavalcante, S. Marques, M.-J. Pindera, Transient Thermomechanical Analysis of a Layered Cylinder by the Parametric Finite-Volume Theory, J. Thermal Stresses 32 (2008) 112–134.
[8] H.S. Carslaw, J.C. Jaeger, Conduction of Heat in Solids, Clarendon Press, Oxford, 1959.
[9] Goodman T.R., "The Adjoint Heat-Conduction Problems for Solids," ASTIA-AD 254–769, (AFOSR-520), April 1961.
[10] V. Vodicka, Eindimensionale wärmeleitung in geschichteten körpern, Math. Nachr. 14 (1955) 47–55.
[11] C.W. Tittle, Boundary-Value Problems in Composite Media: Quasi-Orthogonal Functions, J. Appl. Phys. 36 (1965) 1486–1488.

[12] C.J. Moore, Heat Transfer Across Surfaces in Contact: Studies of Transients in One Dimensional Composite Systems,' Southern Methodist University, Mechanical Engineering Department, Dallas, Texas, 1967 Ph.D. Dissertation.
[13] L. Zhou, M. Parhizi, A. Jain, Temperature distribution in a multi-layer cylinder with circumferentially-varying convective heat transfer boundary conditions,', Int. J. Therm. Sci. 160 (2021) 1–12 106673.
[14] R. Chiba, An analytical solution for transient heat conduction in a composite slab with time-dependent heat transfer coefficient, Mathematical Problems in Engineering, **2018** 4707860 (2018) 1–11.
[15] A. Haji-Sheikh, J.V. Beck, Temperature solution in multi-dimensional multi--layer bodies,', Int. J. Heat Mass Transfer 45 (2002) 1865–1877.
[16] F. de Monte, Unsteady heat conduction in two-dimensional two slab-shaped regions. Exact closed-form solution and results,', Int. J. Heat Mass Transfer 46 (2003) 1455–1469.
[17] H. Salt, Transient heat conduction in a two-dimensional composite slab. II. Physical interpretation of temperatures modes,', Int. J. Heat Mass Transfer 26 (1983) 1617–1623.
[18] M.D. Mikhailov, M.N. Özişik, Transient conduction in a three-dimensional composite slab, Int. J. Heat Mass Transfer 29 (1986) 340–342.
[19] Giuseppe Pontrelli, Filippo de Monte, Modeling of mass dynamics in arterial drug-eluting stents, J. Porous Media 12 (1) (2009) 19–28, doi:10.1615/JPorMedia.v12.i1.20.
[20] M. Doyle, J. Newman, Analysis of capacity–rate data for lithium batteries using simplified models of the discharge process, J. Appl. Electrochem. 27 (1997) 846–856.
[21] M. Parhizi, M.B. Ahmed, A. Jain, Determination of the core temperature of a Li-ion cell during thermal runaway, J. Power Sources 370 (2017) 27–35.
[22] K. Shah, D. Chalise, A. Jain, Experimental and theoretical analysis of a method to predict thermal runaway in Li-ion cells,', J. Power Sources 330 (2016) 167–174.
[23] M. Parhizi, A. Jain, Analytical modeling of solution phase diffusion in porous composite electrodes under time-dependent flux boundary conditions using Green's function method, Ionics, in press (2020), doi:10.1007/s11581-020-03777-1.
[24] P. Huang, et al., Non-dimensional analysis of the criticality of Li-ion battery thermal runaway behavior, J. Hazardous Mater. 369 (2019) 268–278.
[25] R. Spotnitz, J. Franklin, Abuse behavior of high-power, lithium-ion cells,', J. Power Sources 113 (2003) 81–100.
[26] K. Shah, A. Jain, Prediction of thermal runaway and thermal management requirements in cylindrical Li-ion cells in realistic scenarios,', Int. J. Energy Res. 43 (2019) 1827–1838.